Talanta 85 (2011) 1738–1743

Contents lists available at ScienceDirect

Talanta

journal homepage: www.elsevier.com/locate/talanta

Facile synthesis of N-acetyl-L-cysteine capped ZnS quantum dots as an eco-friendly fluorescence sensor for Hg^{2+}

Junling Duan, Xiaochen Jiang, Shouqing Ni, Min Yang, Jinhua Zhan*

Key Laboratory of Colloid and Interface Chemistry, Ministry of Education, Department of Chemistry, Shandong University, Jinan 250100, China

ARTICLE INFO

Article history:
Received 20 April 2011
Received in revised form 24 June 2011
Accepted 27 June 2011
Available online 2 July 2011

Keywords:
Zinc sulfide
Quantum dots
Sensors
Fluorescence
Mercury ions
Nanoparticles

ABSTRACT

This paper described an investigation of a novel eco-friendly fluorescence sensor for Hg^{2+} ions based on N-acetyl-L-cysteine (NAC)-capped ZnS quantum dots (QDs) in aqueous solution. By using safe and low-cost materials, ZnS QDs modified by NAC were easily synthesized in aqueous medium via a one-step method. The quantitative detection of Hg^{2+} ions was developed based on fluorescence quenching of ZnS QDs with high sensitivity and selectivity. Under optimal conditions, its response was linearly proportional to the concentration of Hg^{2+} ions in a range from 0 to 2.4×10^{-6} mol L^{-1} with a detection limit of 5.0×10^{-9} mol L^{-1}. Most of common physiologically relevant cations and anions did not interfere with the detection of Hg^{2+}. The proposed method was applied to the trace determination of Hg^{2+} ions in water samples. The possible quenching mechanism was also examined by fluorescence and UV–vis absorption spectra.

1. Introduction

Much attention has been paid to the environmental contamination with toxic heavy metal ions for decades [1]. Among them, mercury is a well-known dangerous pollutant over the world. Water-soluble inorganic mercuric ion (Hg^{2+}), released from both natural and industrial sources, has severe adverse effects on human health when present in drinking water even at low concentrations [2]. In aquatic sediments, bacteria can convert Hg^{2+} into methylmercury, a potent neurotoxin that can accumulate in the human body through food chain and cause permanent damage to the brain [3–7]. Therefore, the rapid, economical, sensitive and selective detection of trace Hg^{2+} in the environment is extremely important. Up to date, different analytical techniques including atomic absorption spectroscopy [8], cold vapor atomic fluorescence spectrometry [9], inductively coupled plasma mass spectrometry [10] and gas chromatography [11] have been developed to detect Hg^{2+}. As alternative methods, optical sensors, based on changes of spectral absorbance or fluorescence resulting from the interactions between Hg^{2+} and indicators, have been demonstrated to be the simple and quick approach [12–17]. Fluorescence-based sensors, in particular, are extremely attractive because of their intrinsic sensitivity and selectivity [18,19].

So far, a number of fluorescent sensors for Hg^{2+} ions, based on small organic molecules [20–22], biomolecules [23], polymers [24] and foldamers [25], have been reported. Their further applications may be hindered by their complicated synthesis, photo-bleaching or the lack of water solubility. Recently, QDs with water solubility have attracted considerable interest as novel fluorescent sensors. In comparison with traditional organic fluorophores, QDs have unique optical properties such as broad excitation spectra, tunable narrow emission spectra, negligible photo-bleaching and excellent chemical stability, making them more suitable for fluorescent analysis. Since Chen and Rosenzweig first used CdS QDs modified by different ligands as luminescent probes to detect copper and zinc ions in aqueous medium [26], several groups have employed QDs as chemical sensors for cations [27–30] and anions [31–35].

Some QDs-based sensors for Hg^{2+} ions in aqueous medium have been developed. L-Cysteine (L-Cys) [36] and mercaptoacetic acid (MAA) [37] capped CdS QDs and CdS-encapsulated DNA nanocomposite [38] were synthesized for the detection of Hg^{2+}. CdSe QDs modified by triethanolamine (TEA) [39] and L-Cys [40,41] were used for sensing Hg^{2+}. CdTe QDs coated with mercaptopronionic acid (MPA) [42] and denatured bovine serum albumin (dBSA) [43] were utilized for Hg^{2+} analysis. A specific method for Hg^{2+} determination using the fluorescence resonance energy transfer (FRET) between CdTe QDs and butyl-rhodamine B (BRB) was proposed by Li et al. [44]. Liang et al. applied synchronous fluorescence spectroscopy to determine Hg^{2+} with glutathione (GSH)-capped CdS nanoparticles [45]. More recently, Wang et al. reported a Hg^{2+} sensor based on Eu^{3+}-doped CdS composite nanoparticles [46]. Although these

* Corresponding author. Tel.: +86 531 88365017; fax: +86 531 88366280.
E-mail address: jhzhan@sdu.edu.cn (J. Zhan).

0039-9140/$ – see front matter © 2011 Elsevier B.V. All rights reserved.
doi:10.1016/j.talanta.2011.06.071

developed QDs-based sensors for Hg^{2+} provide low detection limits, nearly all of them were based on Cd-chalcogenide QDs (CdS, CdSe, CdTe). Herein, considering the high toxicity of Cd, we developed a novel eco-friendly fluorescence sensor for Hg^{2+} based on Cd-free ZnS QDs with high sensitivity and selectivity. The ZnS QDs were synthesized in aqueous medium via a one-step method. N-acetyl-L-cysteine (NAC), a non-toxic and cost-effective biomolecule [47], is used as stabilizer. The prepared products were water-soluble, biocompatible and low-toxic, which made it possible for NAC-capped ZnS QDs as an eco-friendly fluorescence sensor for Hg^{2+} based on fluorescence quenching of ZnS QDs. The quenching mechanism was examined by fluorescence and UV–vis absorption spectra.

2. Experimental

2.1. Reagents and chemicals

N-acetyl-L-cysteine (NAC) was obtained from Aladdin Chemicals. $Zn(Ac)_2{\cdot}2H_2O$ and $Na_2S{\cdot}9H_2O$ were obtained from Tianjin Chemical Reagent Company. Other analytical grade chemicals were purchased from Shanghai Chemical Reagent Company. All of the chemicals were used as received without further purification. Ultrapure water with 18.2 MΩ/cm was used throughout.

2.2. Characterization of samples

Ultraviolet–visible (UV–vis) absorption spectra were obtained using a TU-1901 UV–vis spectrophotometer (Beijing, China). Photoluminescence (PL) spectra were made with an F-380 spectrofluorimeter (Tianjin, China). The decay time was recorded on an Edinburgh FLS 920 spectrofluorometer, equipped with a 450 W xenon lamp, a 150 W nF900 nanosecond flash lamp with a pulse width of 1 ns and pulse repetition rate of 40–100 kHz. High resolution transmission electron microscopy (HRTEM) images were acquired on a JEM 2100 (JEOL, Japan) electron microscope operating at 200 kV. X-ray diffraction (XRD) patterns were recorded on a Bruker AXS D8 Advance X-ray diffractometer with Cu Kα radiation (λ = 1.5418 Å). The energy-dispersive X-ray spectroscopy (EDS) data was carried out on a JEOL JSM-6700F scanning electron microscope. The pH values were measured with a Model pHS-3C digital pH meter (Shanghai, China). All optical measurements were performed at room temperature under ambient conditions. The quantum yield (QY) of ZnS QDs was determined by using Quinoline sulfate in 0.05 mol L^{-1} H_2SO_4 aqueous solution (QY = 55%) as PL reference [48].

2.3. Synthesis of NAC-capped ZnS QDs

ZnS QDs were synthesized via a one-step method. In a typical synthesis, 1 mL of 0.1 M $Zn(Ac)_2{\cdot}2H_2O$ and 0.0652 g NAC were mixed together in a 100 mL Erlenmeyer flask, then the solution was diluted to 47.5 mL with water. The pH of the mixed solution was adjusted to 10.5 with 2 M NaOH. After that, 1 mL of 0.1 M $Na_2S{\cdot}9H_2O$ was added into the above solution and stirred for 20 min. The final pH of the mixed solution was 10.8 and the total volume was 50 mL. The resulting mixture was aged at 90 °C for 2 h under open-air conditions. The obtained QDs were precipitated with ethanol and redissolved in water for further experiments.

2.4. General procedure for detection of Hg^{2+} ions

The general detection procedure for Hg^{2+} was as follows: into a series of 10 mL colorimetric tubes, 0.4 mL of ZnS QDs stock solution, 0.35 mL of citric acid–Na_2HPO_4 physiological buffer solution (pH 7.2) and different amounts of ions were sequentially added. The mixture was diluted to 5 mL with ultrapure water, shaken thoroughly and equilibrated at room temperature for 15 min. Reference solution was the same without any ions added. The relative fluorescence intensity was measured at $\lambda_{em}/\lambda_{ex}$ = 433/300 nm.

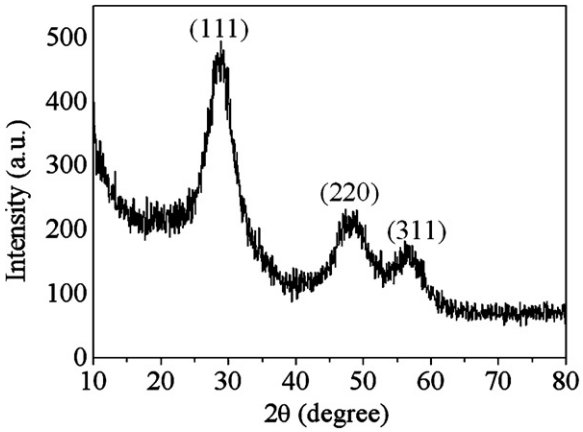

Fig. 1. Typical XRD pattern of ZnS QDs.

3. Results and discussion

3.1. Optimization of ZnS QDs synthesis

To obtain high-quality ZnS QDs, the influences of various synthesis parameters including the precursor concentration, the molar ratio of NAC to Zn^{2+}, the pH of the reaction solution and the reaction time on the fluorescence intensity of ZnS QDs were investigated. ZnS QDs with relatively high fluorescence (QY = 10%) were prepared at 90 °C for 2 h, with the precursor concentration of 2 mM, at NAC to Zn^{2+} molar ratio of 4:1 and pH 10.8. Besides, we also tested different kinds of stabilizers on the fluorescence intensity of ZnS QDs. The stabilizers had a great influence on the fluorescence of ZnS QDs. At the same experimental conditions, NAC-capped ZnS QDs had the optimal fluorescence in comparison with ZnS QDs modified by other stabilizers like L-Cys, GSH, mercaptosuccinic acid (MSA) and MPA (see Fig. S1 in supporting information).

3.2. Characterization of NAC-capped ZnS QDs

A typical XRD pattern for the NAC-capped ZnS QDs is shown in Fig. 1. The powder XRD pattern showed broad peaks typical for nanocrystals. All the reflections were indexed to (1 1 1), (2 2 0), (3 1 1) of the cubic (zinc blende) ZnS (JCPDS No. 65-1691). The average particle size of the product calculated by the Scherrer equation was around 2.7 nm. Fig. 2 provides HRTEM image of as-prepared ZnS QDs, which shows that the obtained ZnS QDs appeared as spherical particles with excellent monodispersity. The average diameter of these nanocrystals was estimated to be 3.0 nm, which was in accordance with the result of XRD.

3.3. Absorption and fluorescence characteristics of NAC-capped ZnS QDs

The absorption and fluorescence spectra of ZnS QDs are shown in Fig. 3. The first absorption peak was located at 290 nm, which blue shifted 50 nm compared to the ZnS bulk phase absorption (340 nm) [49], showing a quantum size effect of the prepared ZnS QDs. The emission peak centered at 433 nm when excited at 300 nm. As shown in the inset image of Fig. 3, the solution of ZnS QDs displayed bright blue fluorescence under a 360 nm UV lamp. The blue

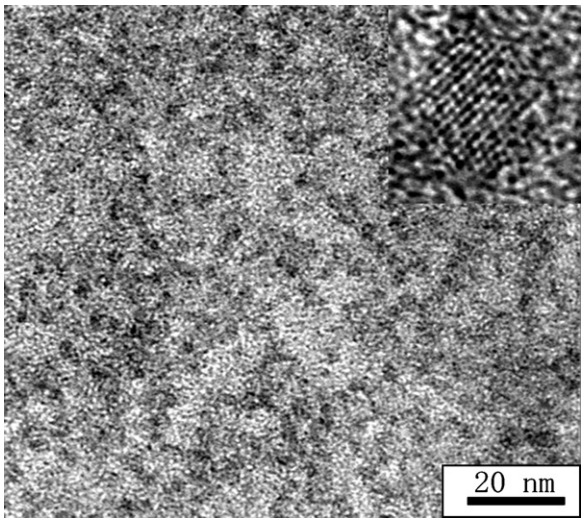

Fig. 2. HRTEM image of ZnS QDs.

emission around 433 nm was attributed to the defect-related emission of ZnS [50].

3.4. Factors affecting the detection of Hg^{2+} ions with NAC-capped ZnS QDs

3.4.1. Effect of reaction time and mixing sequence

According to the experiment, the reaction between ZnS QDs and Hg^{2+} ions reached the equilibrium within 5 min at room temperature, and the fluorescence of ZnS QDs–Hg^{2+} system was stable for at least 1.5 h. Several adding sequences were also tested, indicating that the best order was to mix ZnS QDs, buffer solution first and then Hg^{2+}. The fluorescence signals of the system were recorded after the reaction lasted for 15 min.

3.4.2. Effect of pH and buffer solution

As shown in Fig. 4, the interaction between ZnS QDs and Hg^{2+} was strongly influenced by the pH of the solution. The fluorescence intensity of ZnS QDs was enhanced with the increase of solution pH. The low fluorescence intensity in acid medium might be due to the dissociation of Zn–NAC complexes' annulus owing to the protonation of the surface binding thiolates [51]. With increasing the solution pH, the deprotonation of thiol group in the NAC molecule could strengthen the covalent bond

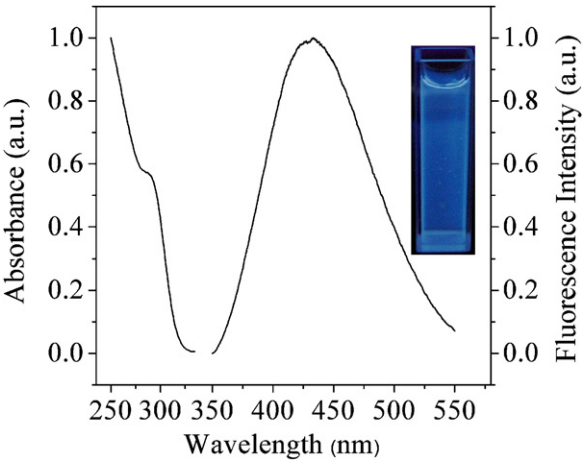

Fig. 3. UV–vis absorption and fluorescence spectra of ZnS QDs. Inset is the optical photo under a 360 nm UV lamp.

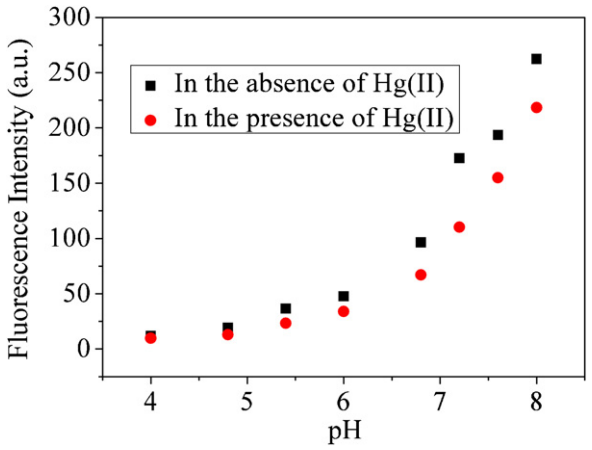

Fig. 4. Effect of pH on the reaction between ZnS QDs and Hg^{2+}. The concentrations of ZnS QDs and Hg^{2+} were 1.6×10^{-4} and 2×10^{-7} mol L^{-1}, respectively.

between NAC and Zn atom on QDs surface, resulting in the increase of fluorescence intensity. The maximum change of fluorescence intensity was observed at a neutral pH 7.2. Meanwhile, the effect of Na_2HPO_4–NaH_2PO_4, KH_2PO_4–NaOH, Tris–HCl and citric acid–Na_2HPO_4 buffer solution was also tested. The optimal buffer solution was citric acid–Na_2HPO_4, and the best buffer volume was 0.35 mL. Therefore, 0.35 mL of pH 7.2 citric acid–Na_2HPO_4 was selected for use in this work.

3.4.3. Effect of ZnS QDs concentration

To obtain the highest sensitivity and the widest linear range of the calibration function, the effect of the concentration of NAC-capped ZnS QDs on the relative fluorescence intensity (F_0/F) of the ZnS QDs–Hg^{2+} system was investigated. The fluorescence intensity increased with the increase of ZnS QDs concentration (not shown). Higher QDs concentration could increase the linear range but reduce the sensitivity. As shown in Fig. 5, the maximum F_0/F was achieved when the concentration was 1.6×10^{-4} mol L^{-1}. Considering both high sensitivity and wide linear range, 1.6×10^{-4} mol L^{-1} was recommended for further research.

3.4.4. Effect of foreign ions

The effect of different biologically relevant cations (Fig. S2A) and anions (Fig. S2B) on the fluorescence of NAC-capped ZnS QDs was systematically conducted to evaluate the selectivity. Fig. S2A shows that Hg^{2+} displayed the strongest fluorescence quenching

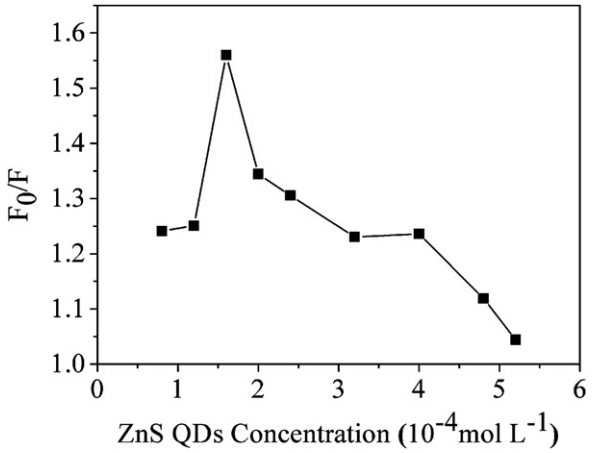

Fig. 5. Effect of ZnS QDs concentration on the relative fluorescence intensity (F_0/F) of ZnS QDs–Hg^{2+} system. The Hg^{2+} concentration was 2×10^{-7} mol L^{-1}.

Table 1
Test for the interference of different cations and anions on the fluorescence of NAC-capped ZnS QDs at pH 7.2.

Coexisting substance	Coexisting concentration (10^{-7} mol L^{-1})	Relative error (%)	Coexisting substance	Coexisting concentration (10^{-7} mol L^{-1})	Relative error (%)
Na^+	4000	+4.3	F^-	4000	+4.3
Mg^{2+}	3000	−4.7	Cl^-	4000	+4.3
Ca^{2+}	4000	−4.6	I^-	4000	+0.8
Sr^{2+}	1000	+3.0	S^{2-}	4000	+0.5
Ba^{2+}	600	−3.5	$S_2O_8^{2-}$	4000	+4.5
Fe^{3+}	400	+1.6	SO_3^{2-}	4000	+0.1
Co^{2+}	1600	+3.2	HPO_4^{2-}	4000	+3.7
Ni^{2+}	1600	+2.8	Ac^-	4000	+2.8
Mn^{2+}	2000	−2.4	HCO_3^-	4000	+3.5
Cu^{2+}	5	−4.2	ClO_4^-	4000	+2.7
Ag^+	40	−3.2	CO_3^{2-}	4000	+3.8
Zn^{2+}	1600	+1.4	NO_3^-	4000	+5.0

Concentration of Hg^{2+} ion: 1.0×10^{-7} mol L^{-1}. Other conditions are the same as those described in the procedure.

of ZnS QDs, and Cu^{2+} could minimally quench the fluorescence, while other ions scarcely had effect on the fluorescence of ZnS QDs. Meanwhile, the fluorescence titration of NAC-capped ZnS QDs with various coexisting ions was conducted to further examine the interference of foreign ions in the determination of Hg^{2+} ions (1.0×10^{-7} mol L^{-1}). As shown in Table 1, relatively high concentrations of alkali, alkaline earth, etc. cations did not cause interference, only Cu^{2+} can be tolerated with relatively low concentrations. Halogen anions, CO_3^{2-}, NO_3^-, etc. anions showed slight interference at 4000-fold higher than the concentration of Hg^{2+}. The experimental results showed that most of the examined coexisting ions hardly interfered with the Hg^{2+} determination.

3.5. Analytical performance of NAC-capped ZnS QDs

The effect of Hg^{2+} concentration on the fluorescence of NAC-capped ZnS QDs is shown in Fig. 6A. The fluorescence intensity of NAC-capped ZnS QDs was dramatically decreased with increase of Hg^{2+} concentration. So a quantitative detection of Hg^{2+} ions based on fluorescence quenching was possible. It was further found that the quenching effect of Hg^{2+} on the fluorescence of ZnS QDs was concentration-dependent and the fluorescence quenching data fitted Stern–Volmer-type relationship, which was given by the following equation:

$$\frac{F_0}{F} = 1 + K_{SV}[C]$$

F and F_0 are the fluorescence intensities of ZnS QDs in the presence and absence of Hg^{2+} respectively, [C] is the Hg^{2+} concentration, and K_{SV} is the Stern–Volmer quenching constant. Fig. 6B shows the Stern–Volmer plot describing F_0/F as a function of Hg^{2+} concentration. The K_{SV} was found to be 3.76×10^6 L mol^{-1}. A good linear relationship was observed at the Hg^{2+} concentration from 0 to 2.4×10^{-6} mol L^{-1} with a correlation coefficient of 0.9985. The limit of detection (LOD), calculated following the 3σ IUPAC criteria, was 5.0 nM. The relative standard deviation of six replicate measurements for solution containing 1.0×10^{-7} mol L^{-1} Hg^{2+} ion was 2.5%. It can be seen that the proposed method had a comparable or superior linear range and detection limit compared with the current used Cd-chalcogenide QDs-based sensors for Hg^{2+} detection, the analytical results of some QDs-based sensors for the determination of Hg^{2+} are summarized in Table 2.

To evaluate the practical application of the developed method, the ZnS QDs-based sensor was applied to determine Hg^{2+} ions in tap water and spring water samples. Mercury in water GBW(E)080701 as certified reference material was analyzed by this method. The results are shown in Table 3. It can be found that the results of recovery for water samples were satisfied and the concentrations of Hg^{2+} determined by the proposed method were in good agreement with those obtained by cold vapor atomic fluorescence spectrometry (CV-AFS), suggesting this method was reliable and practical for detecting Hg^{2+} ions in aqueous environment.

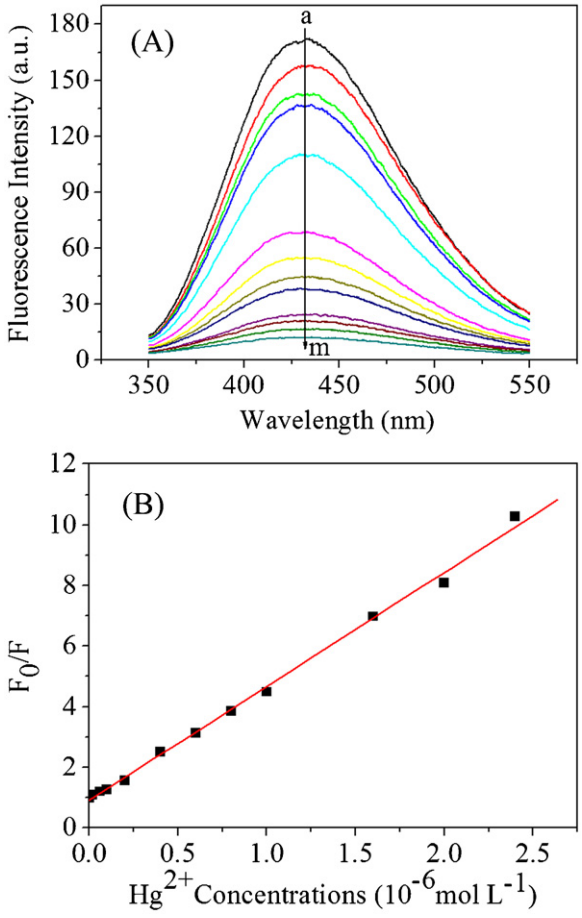

Fig. 6. (A) Effect of Hg^{2+} concentration on the fluorescence of ZnS QDs and (B) Stern–Volmer plot of the fluorescence intensity of ZnS QDs vs. the Hg^{2+} concentration. The concentrations of Hg^{2+} (a–m, $\times 10^{-6}$ mol L^{-1}) were: 0, 0.02, 0.06, 0.1, 0.2, 0.4, 0.6, 0.8, 1.0, 1.6, 2.0, 2.4, 3.0.

3.6. Possible mechanism of quenching

Up to now, many quenching mechanisms including electron transfer process, ion binding interaction, inner filter effect and non radiative recombination pathway have been proposed to explain the quenching phenomena of QDs [26,36,42]. In general, two mechanisms were proposed to explain the quenching effect of Hg^{2+} on

Table 2
Comparison of analytical performance of QDs-based sensors for Hg^{2+} detection.

Reagents	$\lambda_{ex}/\lambda_{em}$ (nm)	Linear range ($\times10^{-7}$ mol L^{-1})	LOD ($\times10^{-9}$ mol L^{-1})
MAA-capped CdS QDs [37]	360/495	0.05–4	4.2
L-Cys-capped CdSe QDs [40]	430/530	0–20	6.0
dBSA-capped CdTe QDs [43]	380/541	0.12–15	4.0
CdTe–BRB FRET system [44]	447/576	0.625–25	20.3
NAC-capped ZnS QDs	300/433	0–24	5.0

Table 3
Analytical results for the determination of Hg^{2+} in tap water samples using NAC-capped ZnS QDs.

Samples	Certified value (μg/mL)	This method (μg/mL) $n=5$	Hg(II) added (10^{-6} mol L^{-1})	Hg(II) founded (10^{-6} mol L^{-1})[a]		Recovery (%)	RSD (%)
				This method	CV-AFS		
GBW(E)080701	0.100	0.104					1.2
Tab water			0.2	0.19	0.22	95.0	3.0
			0.4	0.405	0.41	101.3	2.8
Spring water			0.2	0.189	0.182	94.5	2.1
			0.4	0.392	0.39	98.0	2.4

[a] The average of five replicate determinations.

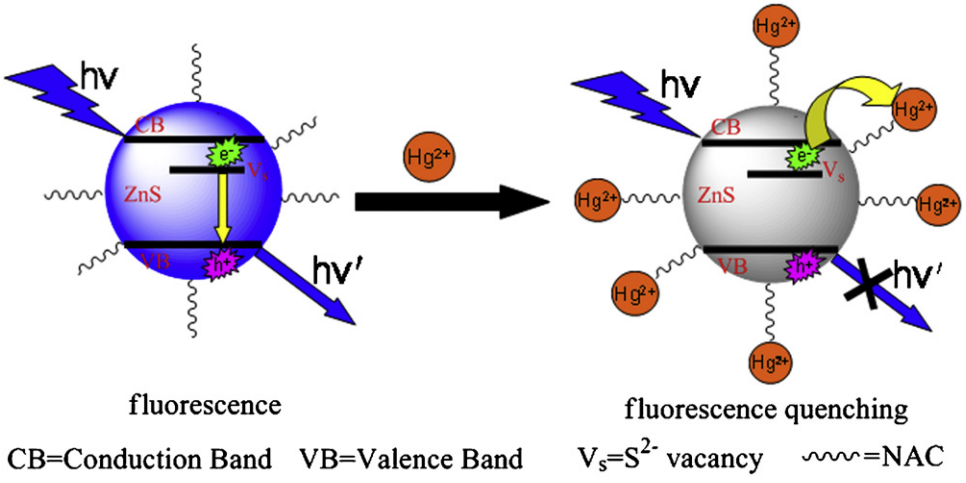

Scheme 1. Schematic illustration for the fluorescence quenching of NAC-capped ZnS QDs by Hg^{2+}.

QDs fluorescence. For example, Yan et al. reported that the fluorescence quenching of CdS QDs by Hg^{2+} was due to the formation of HgS particles. Owing to the lower solubility of HgS compared with CdS, HgS particles were formed through the displacement of Cd(II) by Hg(II) on QDs surface, leading to a red shift of the absorption peak [36]. On the other hand, Zhu et al. demonstrated that Hg^{2+} quenched the fluorescence of QDs through an electron transfer process between surface ligands and Hg^{2+} without spectra shift [40–42]. In our study, the quenching mechanism was studied by fluorescence and UV–vis absorption spectra. As illustrated in Fig. 6A, the fluorescence intensity of ZnS QDs was quenched without spectra shift in the presence of Hg^{2+}. To further understand the quenching effect, UV–vis absorption spectra of ZnS QDs in the absence and presence of Hg^{2+} ions were investigated. As shown in Fig. 7, no shift was observed in the absorption peak of ZnS QDs with addition of Hg^{2+}. The fluorescence quenching of ZnS QDs, with no spectra shift in both absorption and emission peaks in the presence of Hg^{2+}, was in accordance with the latter literature discussed above. Meanwhile, XRD and EDS of ZnS QDs after addition of Hg^{2+} ions were performed. The diffraction patterns before and after addition of Hg^{2+} were identical (Fig. S3) and there was no Hg element found in EDS data (Fig. S4), indicating HgS particles were not formed in our system. The quenching mechanism was assumed to be the effective electron transfer from surface traps of ZnS QDs to Hg^{2+} ions. Hg^{2+} ion, being one of the "soft" metal ions, had strong affinity with the carboxyl and amido groups of NAC on the surface of ZnS QDs. The electron transfer between ZnS QDs and Hg^{2+} resulted in the fluorescence quenching of ZnS QDs by facilitating nonradiative

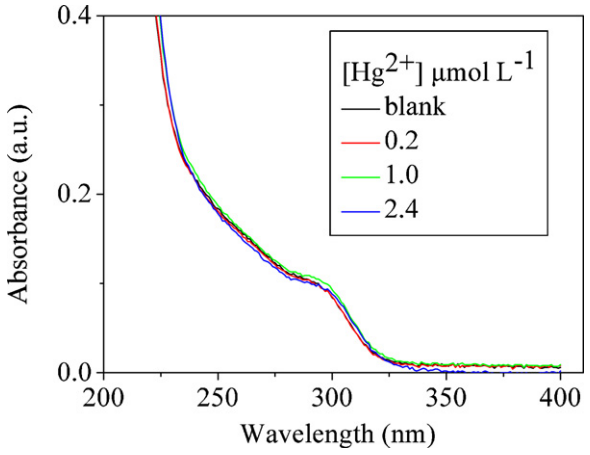

Fig. 7. UV–vis absorption spectra of ZnS QDs in the absence and presence of different concentrations of Hg^{2+}.

recombination of excited electrons (e^-) in the S^{2-}-vacancy-related band and holes (h^+) in the valence band. The quenching mechanism is shown in Scheme 1. To further confirm the quenching mechanism, the fluorescence decay profiles of ZnS QDs at different concentrations of Hg^{2+} were recorded, and the decays were fitted with the equation of $I(t) = A_1 \exp(-t/\tau_1) + A_2 \exp(-t/\tau_2)$ (as shown in Table S1). The fluorescence lifetimes of ZnS QDs were decreased with addition of Hg^{2+}, which may result from the electron transfer from surface traps of ZnS QDs to Hg^{2+}.

4. Conclusions

A novel eco-friendly fluorescence sensor for Hg^{2+} with high sensitivity and selectivity was developed using health-friendly ZnS QDs as a fluorescent probe. Water-soluble ZnS QDs capped with NAC were easily synthesized by a one-step process. The factors affecting both the synthesis of NAC-capped ZnS QDs and the fluorescence detection for Hg^{2+} were tested. Under optimal conditions, relatively wide linear range (from 0 to 2.4×10^{-6} mol L^{-1}) and low detection limit (5.0×10^{-9} mol L^{-1}) were obtained. Most common coexisting cations and anions hardly interfered with the determination of Hg^{2+}. The concentration-dependent fluorescence quenching could be described by Stern–Volmer equation and the quenching mechanism was attributed to the effective electron transfer from surface traps of QDs to Hg^{2+} ions. The proposed method was applied to the recognition of Hg^{2+} ions in real water samples.

Acknowledgements

Financial support from National Natural Science Foundation of China (NSFC 50972083 and 21075077), Independent Innovation Foundation of Shandong University (IIFSDU-2009JQ011), the Key Project of Chinese Ministry of Education (No. 109098), National Basic Research Program of China (973 Program 2007CB936602) and Shandong Provincial Natural Science Foundation for Distinguished Young Scholar (JQ201004) is gratefully acknowledged.

Appendix A. Supplementary data

Supplementary data associated with this article can be found, in the online version, at doi:10.1016/j.talanta.2011.06.071.

References

[1] D.W. Boening, Chemosphere 40 (2000) 1335–1351.
[2] T.W. Clarkson, L. Magos, G.J. Myers, N. Engl. J. Med. 349 (2003) 1731–1737.
[3] W. Zheng, M. Aschner, J.F. Ghersi-Egea, Toxicol. Appl. Pharmacol. 192 (2003) 1–11.
[4] D.P. Wojcik, M.E. Godfrey, D. Christie, B.E. Haley, Neuroendocrinol. Lett. 27 (2006) 415–423.
[5] B.K. Jena, C.R. Raj, Anal. Chem. 80 (2008) 4836–4844.
[6] E.M. Nolan, S.J. Lippard, Chem. Rev. 108 (2008) 3443–3480.
[7] H.H. Harris, I.J. Pickering, G.N. George, Science 301 (2003) 1203.
[8] Y.A. Vil'pan, I.L. Grinshtein, A.A. Akatove, S. Gucer, J. Anal. Chem. 60 (2005) 38–44.
[9] L.P. Yu, X.P. Yan, Atom. Spectrosc. 25 (2004) 145–153.
[10] J.A. Moreton, H.T. Delves, J. Anal. Atom. Spectrom. 13 (1998) 659–665.
[11] W.F. Fitzgerald, G.A. Gill, Anal. Chem. 51 (1979) 1714–1720.
[12] C.C. Huang, Z. Yang, K.H. Lee, H.T. Chang, Angew. Chem. Int. Ed. 46 (2007) 6824–6828.
[13] H. Wei, Z.D. Wang, L.M. Yang, S.L. Tian, C.J. Hou, Y. Lu, Analyst 135 (2010) 1406–1410.
[14] D.H. Hu, Z.H. Sheng, P. Gong, P.F. Zhang, L.T. Cai, Analyst 135 (2010) 1411–1416.
[15] J.S. Lee, M.S. Han, C.A. Mirkin, Angew. Chem. Int. Ed. 46 (2007) 4093–4096.
[16] G.K. Darbha, A. Ray, P.C. Ray, ACS Nano 1 (2007) 208–214.
[17] G.K. Darbha, A.K. Singh, U.S. Rai, E. Yu, H.T. Yu, P.C. Ray, J. Am. Chem. Soc. 130 (2008) 8038–8043.
[18] R.H. Yang, K.A. Li, K.M. Wang, F.L. Zhao, N. Li, F. Liu, Anal. Chem. 75 (2003) 612–621.
[19] R.H. Yang, Y. Zhang, K.A. Li, F. Liu, W.H. Chan, Anal. Chim. Acta 525 (2004) 97–103.
[20] B. Liu, H. Tian, Chem. Commun. 25 (2005) 3156–3158.
[21] M.H. Lee, J.S. Wu, J.W. Lee, J.H. Jung, J.S. Kim, Org. Lett. 9 (2007) 2501–2504.
[22] E.M. Nolan, S.J. Lippard, J. Am. Chem. Soc. 129 (2007) 5910–5918.
[23] J. Liu, Y. Lu, Angew. Chem. Int. Ed. 46 (2007) 7587–7590.
[24] L.J. Fan, Y. Zhang, W.E. Jones, Macromolecules 38 (2005) 2844–2849.
[25] Y. Zhao, Z.Q. Zhong, J. Am. Chem. Soc. 128 (2006) 9988–9989.
[26] Y.F. Chen, Z. Rosenzweig, Anal. Chem. 74 (2002) 5132–5138.
[27] C.Y. Chen, C.T. Cheng, C.W. Lai, P.W. Wu, K.C. Wu, P.T. Chou, Y.H. Chou, H.T. Chiu, Chem. Commun. 3 (2006) 263–265.
[28] K.M. Gattás-Asfura, R.M. Leblanc, Chem. Commun. 21 (2003) 2684–2685.
[29] E.M. Ali, Y.G. Zheng, H.H. Yu, J.Y. Ying, Anal. Chem. 79 (2007) 9452–9458.
[30] M. Koneswaran, R. Narayanaswamy, Sens. Actuators B 139 (2009) 104–109.
[31] W.J. Jin, M.T. Fernández-Argüelles, J.M. Costa-Fernández, R. Pereiro, A. Sanz-Medel, Chem. Commun. 7 (2005) 883–885.
[32] C.L. Wu, Y.B. Zhao, Anal. Bioanal. Chem. 388 (2007) 717–722.
[33] X. Liu, L. Guo, L.X. Cheng, H.X. Ju, Talanta 78 (2009) 691–694.
[34] R.C. Mulrooney, N. Singh, N. Kaur, J.F. Callan, Chem. Commun. 6 (2009) 686–688.
[35] B.H. Zhang, F.Y. Wu, Y.M. Wu, X.S. Zhan, J. Fluoresc. 20 (2010) 243–250.
[36] Z.X. Cai, H. Yang, Y. Zhang, X.P. Yan, Anal. Chim. Acta 559 (2006) 234–239.
[37] M. Koneswaran, R. Narayanaswamy, Sens. Actuators B 139 (2009) 91–96.
[38] Y.F. Long, D.L. Jiang, X. Zhu, J.X. Wang, F.M. Zhou, Anal. Chem. 81 (2009) 2652–2657.
[39] Z.B. Shang, Y. Wang, W.J. Jin, Talanta 30 (2009) 364–369.
[40] J.L. Chen, Y.C. Gao, Z.B. Xu, G.H. Wu, Y.C. Chen, C.Q. Zhu, Anal. Chim. Acta 577 (2006) 77–84.
[41] J.L. Chen, Y.C. Gao, C. Guo, G.H. Wu, Y.C. Chen, B.W. Lin, Spectrochim. Acta A 69 (2008) 572–579.
[42] B. Chen, Y. Yu, Z.T. Zhou, P. Zhong, Chem. Lett. 33 (2004) 1608–1609.
[43] Y.S. Xia, C.Q. Zhu, Talanta 75 (2008) 215–221.
[44] J. Li, F. Mei, W.Y. Li, X.W. He, Y.K. Zhang, Spectrochim. Acta A 70 (2008) 811–817.
[45] A.N. Liang, L. Wang, H.Q. Chen, B.B. Qian, B. Ling, J. Fu, Talanta 81 (2010) 438–443.
[46] H.Q. Chen, J. Fu, L. Wang, B. Ling, B.B. Qian, J.G. Chen, C.L. Zhou, Talanta 83 (2010) 139–144.
[47] E. Raspanti, S.O. Cacciola, C. Gotor, L.C. Romero, I. García, Chemosphere 76 (2009) 48–54.
[48] G.A. Crosby, J.N. Demas, J. Phys. Chem. 75 (1971) 991–1024.
[49] J.Q. Zhuang, X.D. Zhang, G. Wang, D.M. Li, W.S. Yang, T.J. Li, J. Mater. Chem. 13 (2003) 1853–1857.
[50] J.F. Suyver, S.F. Wuister, J.J. Kelly, A. Meijerink, Nano Lett. 1 (2001) 429–433.
[51] M.Y. Gao, S. Kirstein, H. Möhwald, A.L. Rogach, A. Kornowski, A. Eychmü ller, H. Weller, J. Phys. Chem. B 102 (1998) 8360–8363.